Surface Deformation along the Carmel-Gilboa Fault System by means of Extended Free Network Adjustment Constraints

Gilad EVEN-TZUR, Israel

Key words: Deformation, GPS, Velocity Field, Extended Free Network, Datum.

SUMMARY

The Carmel-Gilboa Fault System is one of the major geological structures of northern Israel. It is a northwestern branch of the Dead Sea Fault. Tectonic activity and crustal deformation occurs along the Carmel Gilboa Fault System. The fault system region is covered by a monitoring geodetic network consisting of 24 sites. In this paper we analyze GPS data which were measured eight times between 1999 and 2016 and derive regional velocities for the network sites. The site velocities were estimated with respect to a local datum by means of extended free network adjustment constraints.

In this study the GPS vectors from each campaign are stripped from their datum content using the extended free network adjustment constraints. The datumless measurements are used to define the datum by preliminary coordinates and linear constraints, which remain constant for all monitoring campaigns, as well as to define the position of the network points and their velocities. The use of extended S-transformation enables transition from one datum to another and calculates the velocities in relation to the chosen datum.

The horizontal velocity field shows deformations of about 1 mm/yr sinistral which is not contradictory to previous geophysical studies. But, a careful examination of the velocity field raises doubts about the location of the fault system today.

Surface Deformation Along the Carmel-Gilboa Fault System by Means of Extended Free Network Adjustment Constraints (9976)
Gilad Even-Tzur (Israel)

FIG Working Week 2019
Geospatial information for a smarter life and environmental resilience
Hanoi, Vietnam, April 22–26, 2019

Surface Deformation along the Carmel-Gilboa Fault System by means of Extended Free Network Adjustment Constraints

Gilad EVEN-TZUR, Israel

1. INTRODUCTION

The Carmel-Gilboa Fault System (CGFS) is one of the major geological structures of northern Israel. It is a northwestern branch of the Dead Sea Fault (DSF). The DSF is a left-lateral transform that forms the boundary between the Arabian Plate and the Sinai Sub-Plate mainly on the N-S trending (Fig 1). The CGFS is composed of several NW-SE trending faults while the main faults are the Carmel Fault (CF) and Gilboa Fault (GF) (Fig. 2). The CGFS starts at the Jordan Valley, goes up to the northern tip of Mount Carmel and extends into the Mediterranean Sea (Fig. 2).
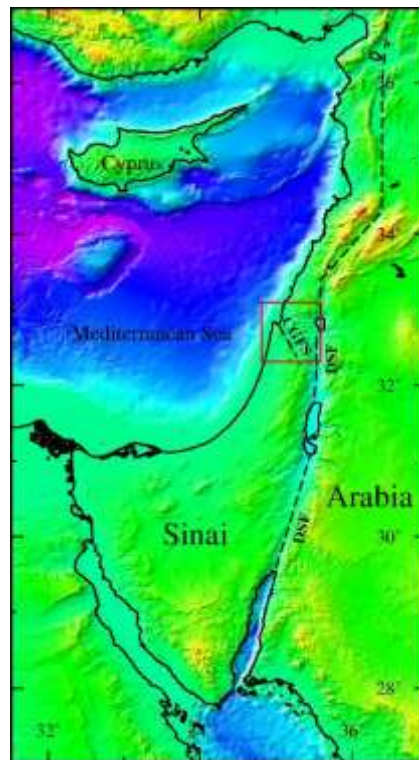

Figure 1. Tectonic map of Eastern Mediterranean showing the Sinai and Arabia plates. The black dash line denotes the location of the Dead Sea Fault (DSF). The red box denotes the study area with the Carmel Gilboa Fault System (CGFS) location.

Surface Deformation Along the Carmel-Gilboa Fault System by Means of Extended Free Network Adjustment Constraints (9976)
Gilad Even-Tzur (Israel)

FIG Working Week 2019
Geospatial information for a smarter life and environmental resilience
Hanoi, Vietnam, April 22–26, 2019

There is no agreement on the exact location of the CGFS. There are those who locate the main fault along the southwestern side of the Yizre'el Valley (for example, Hofstetter et al., 1996; Rotstein et al., 2004; Fleischer and Gafsou, 2005) and others locate the main fault somewhere within the Yizre'el Valley downfaulted structure (Segev and Rybakov, 2011). Actually, the CGFS is a wide (up to ~20 km) deformation zone on the valley's southeastern side, which narrows towards the northwest (Mount Carmel). The fault pattern within the Yizre'el Valley is not well known. Some suggested a fault system below the Yizre'el Valley, which connects the Gilboa and the Carmel faults (Segev et al., 2006; Segev et al., 2014).

Mount Carmel is an elevated and intensively faulted area that is bordered by the main Carmel Fault on the northeast. The latter is divided into two main segments: A NW-SE oriented segment that runs from Haifa Bay towards Amaqim Junction (Jalame) and a N-S oriented fault that runs between Jalame and Yoqneam (Fig. 2). Its continuation southward is the Yoqneam Fault.

In this study we implement the extended free network adjustment constraints solution to calculate the velocities of 24 sites that were measured eight times between 1999 and 2016 using GPS. The outcome is a velocity field covering the Carmel Fault region. Since the accuracy of vertical position is low relative to horizontal position, we only estimated the horizontal site velocities. The local datum is taken into account by extended similarity transformation, that allows for transforming the coordinates of network sites to any desired datum.
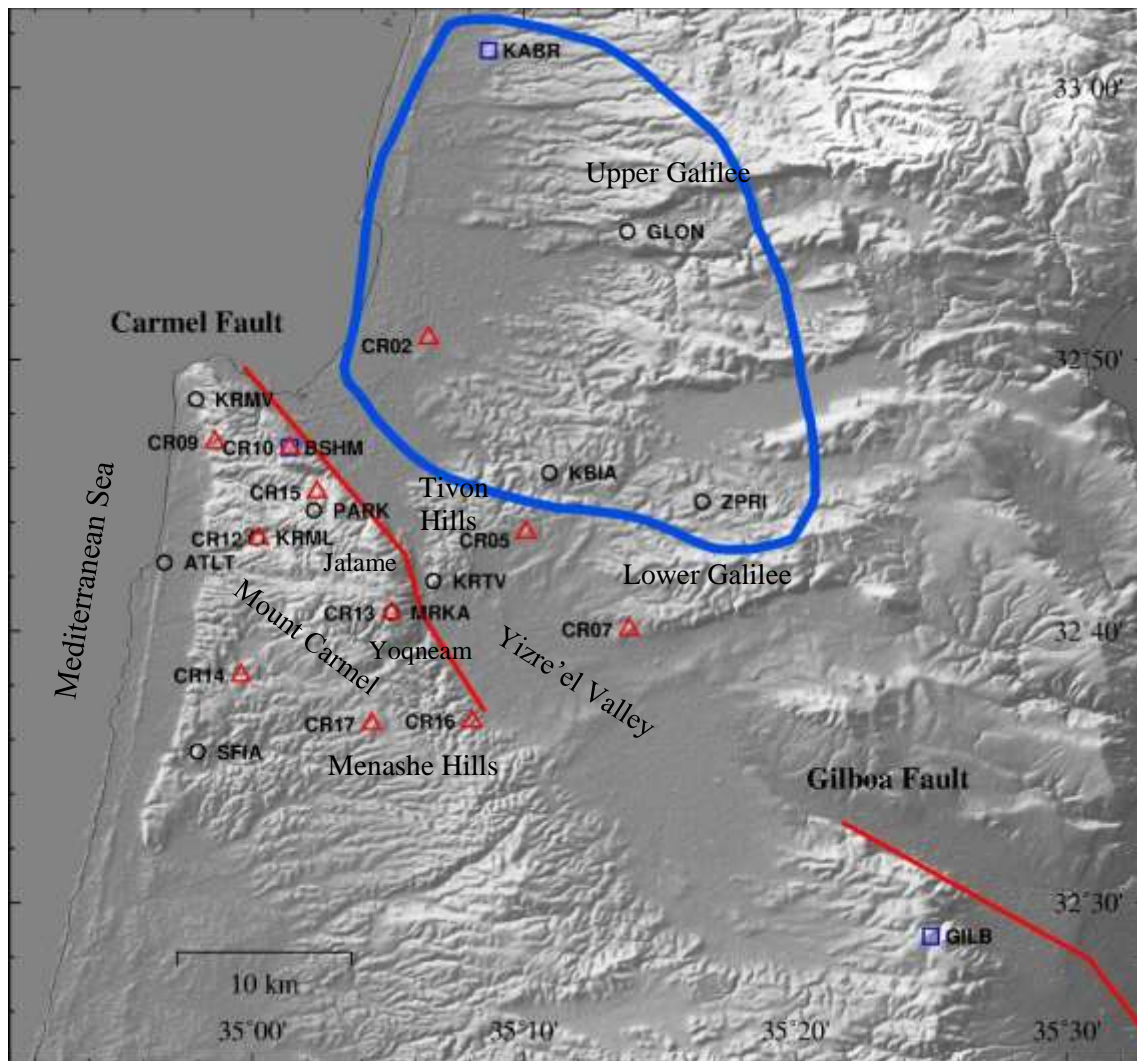
Surface Deformation Along the Carmel-Gilboa Fault System by Means of Extended Free Network Adjustment Constraints (9976)
Gilad Even-Tzur (Israel)

FIG Working Week 2019
Geospatial information for a smarter life and environmental resilience
Hanoi, Vietnam, April 22–26, 2019

Figure 2. The digital elevation map of the study area with the location of the Carmel Gilboa Fault System and GPS sites used in this analysis. Blue squares: APN sites. Black circles: G1 sites. Red triangles: CR sites. The Blue line denote the Galilee datum points.

2. THE GPS NETWORK, CAMPAIGNS AND DATA PROCESSING

The CGFS region is covered by a geodetic monitoring network, consisting of 24 sites (Fig. 2) that were measured in 1999, 2006, 2009, 2010, 2011, 2012, 2014 and 2016 by means of GPS. The network that was used to determine the velocity field consists of three parts that are combined in observation and analysis: The Carmel network, the G1 network and three sites of the Israeli network of permanent GNSS sites (APN, Active Permanent Network). The Carmel network (CR) was established in 1990 to monitor horizontal movements in the Carmel region. Today the network is composed of 11 points (Fig. 2, red triangles). The network points were

Surface Deformation Along the Carmel-Gilboa Fault System by Means of Extended Free Network Adjustment Constraints (9976)
Gilad Even-Tzur (Israel)

FIG Working Week 2019
Geospatial information for a smarter life and environmental resilience
Hanoi, Vietnam, April 22–26, 2019

marked, without any exception, on exposed and solid bedrock. The G1 network was designed and established in the beginning of the 1990s with the intention of monitoring crustal deformation and serving as the major control network in Israel. The marks were built according to high technical specifications to ensure their geotechnical stability. Ten G1 sites were measured (Fig. 2, black circles), two of them are located close to two sites of CR, enabling a double check of the resulting site velocities. Additionally, data from seven sites (ELAT, RAMO, TELA KATZ, BSHM, KABR and GILB) of the Israeli network of permanent GPS sites (APN) and three supplementary IGS sites (NICO, ANKR and ZECK) are included in the GPS analysis. Three of the APN sites (Fig. 2, blue squares) are in the vicinity of the network and therefore are incorporated in the deformation analysis. One of the sites (BSHM) is close to another CR network site.

The non-permanent sites were occupied using tripods for the CR network sites while the G1 network sites were measured using special centering devices, which allow an easier setup of the antenna. All sites were occupied at least twice in each campaign with observation time spans of 4 h for the 1999 campaign and 8 h for all the other campaigns (2006 until 2016). In all campaigns dual-frequency receivers were used. In 1999 and 2006 campaigns choke ring antennas were used along with geodetic antennas, since 2009 choke ring antennas were used exclusively.

In total, GPS data from 31 sites were incorporated into the analysis process. The GPS data analysis was done using the Bernese GNSS Software Version 5.2 (Dach et al., 2015). All campaigns were processed using precise ephemeris, EOPs and absolute antenna phase center variations with respect to IGS08 (http://igscb.jpl.nasa.gov). To ensure the consistency of all campaign solutions we introduced the IGS coordinates from the weekly solution for IGS stations as approximate coordinates. The datum was defined by loose constraints of the IGS site coordinates. This reduced the influence of possible seasonal variations of site coordinates which are not covered by linear IGS velocities.

3. VELOCITY FIELD ESTIMATION

The site velocities can be estimated only if the datum of the network has not been changed between measurement epochs. The GPS vectors must be adjusted so that the datum will remain

Surface Deformation Along the Carmel-Gilboa Fault System by Means of Extended Free Network Adjustment Constraints (9976)
Gilad Even-Tzur (Israel)

FIG Working Week 2019
Geospatial information for a smarter life and environmental resilience
Hanoi, Vietnam, April 22–26, 2019

undisturbed throughout the measurement campaigns. Usually we assume that GPS vectors define the network datum components of orientation and scale. Fluctuations in the GPS orbits could affect the orientation and scale between monitoring campaigns and therefore we assume that GPS vectors are not immune to changes in their datum content. An appropriate approach is taken to prevent the inclusion of these components in the adjustment of a 4D network. If not, the result will be an inevitable mixture between the deformation parameters and the datum components of the GPS vectors.

The GPS vectors from each campaign are stripped from their datum content using the extended free network adjustment constraints. The datumless measurements are used to define the datum by preliminary coordinates and linear constraints, which remain constant for all monitoring campaigns, as well as to define the position of the network points and theirs velocities. Later, the variations in the network geometry can be modeled by means of a physical model.

4. EXTENDED FREE NETWORK ADJUSTMENT CONSTRAINTS

The relationship between a vector of n measurements ℓ and a vector of u parameters $\mathbf{w}$ can be expressed by a set of observation equations given as:

$$\ell + \mathbf{v} = \mathbf{Cw} \qquad (1)$$

$\mathbf{C}$ denotes the design matrix and $\mathbf{v}$ is the vector of measurement corrections. It may be assumed that $\mathbf{C}$ is column rank deficient due to the need for datum definition.

The vector $\mathbf{w}$ is partitioned into global and local components through the introduction of a vector of parameters $\mathbf{y}$ (Papo, 1985). Let us denote $\mathbf{x}$ as a vector of sterilized coordinates. $\mathbf{x}$ represents a coordinate where the global content of the measurements has been withheld.

The elements of $\mathbf{y}$ can be related as the parameters of a transformation (mapping function) between the two vectors $\mathbf{x}$ and $\mathbf{w}$ and contain f parameters. The differences between $\mathbf{x}$ and $\mathbf{w}$ are the characteristics represented by the transformation and the parameters $\mathbf{y}$. Therefore $\mathbf{w}$ can be presents as

$$\mathbf{w} = \mathbf{Dx} + \mathbf{Fy} \qquad (2)$$

where $\mathbf{D} = \partial \mathbf{w}/\partial \mathbf{x}$ is a $u \times u$ full rank matrix called the deformation matrix, and $\mathbf{F} = \partial \mathbf{w}/\partial \mathbf{y}$ is a $u \times f$ matrix of full column rank. Now, the observation equations (1) are rewritten as,

Surface Deformation Along the Carmel-Gilboa Fault System by Means of Extended Free Network Adjustment Constraints (9976)
Gilad Even-Tzur (Israel)

FIG Working Week 2019
Geospatial information for a smarter life and environmental resilience
Hanoi, Vietnam, April 22–26, 2019

$$\ell + \mathbf{v} = \mathbf{C}(\mathbf{D}\mathbf{x} + \mathbf{F}\mathbf{y}) = \mathbf{C}(\mathbf{D}, \mathbf{F})\begin{bmatrix} \mathbf{x} \\ \mathbf{y} \end{bmatrix} = (\mathbf{A}, \mathbf{B})\begin{bmatrix} \mathbf{x} \\ \mathbf{y} \end{bmatrix}. \tag{3}$$

The solution of $\mathbf{x}$ and $\mathbf{y}$ and their cofactor matrix by means of extended free net adjustment constraints were presented by Papo (1985, 1986) and Even-Tzur (2011).

5. EXTENDED S-TRANSFORMATION

In geodetic monitoring networks the similarity transformation is a powerful tool. It enables bringing all monitoring campaigns to the same common datum. The similarity transformation operation is used for transition from one datum to another without using a new adjustment computation. The transition is done on the coordinates or velocities and on their variance covariance matrixes.

The known S-transformation (Baarda, 1973) should be fitted into an extended free net adjustment. According to Wolf (1977) we can transform one solution of $\mathbf{x}$ and $\mathbf{y}$, pertaining to a certain datum, into another solution $\bar{\mathbf{x}}$ and $\bar{\mathbf{y}}$ pertaining to another datum, using an extended similarity transformation. Let $\mathbf{E}$ be the Helmert transformation matrix, $\mathbf{p}$ a vector of d datum transformation parameters and $\mathbf{q}$ a vector of f variations in the $\mathbf{y}$ parameters. $\mathbf{R}$ is a $u \times f$ matrix of full column rank that represents an apparent functional relationship between $\mathbf{x}$ and $\mathbf{y}$, $\mathbf{R} = -\mathbf{D}^{-1}\mathbf{F}$ (Papo, 1985). The transformation is described by:

$$\begin{aligned} \bar{\mathbf{x}} &= \mathbf{x} + \mathbf{D}^{-1}\mathbf{E}\mathbf{p} + \mathbf{R}\mathbf{q} \\ \bar{\mathbf{y}} &= \mathbf{y} + \mathbf{q} \end{aligned} \tag{4}$$

Let $\mathbf{P}_x$ be a diagonal matrix with 1 for points that enter the datum definition and 0 for all others. Therefore, in order to bring about a unique solution of $\bar{\mathbf{x}}$ that yields $\bar{\mathbf{x}}^T\mathbf{P}_x\bar{\mathbf{x}}$ to be minimal, it is required that $\partial(\bar{\mathbf{x}}^T\mathbf{P}_x\bar{\mathbf{x}})/\partial\mathbf{p} = 0$ and $\partial(\bar{\mathbf{x}}^T\mathbf{P}_x\bar{\mathbf{x}})/\partial\mathbf{q} = 0$. If $\mathbf{I}$ is the identity matrix the transformation will receive the following form (Even-Tzur, 2012):

$$\bar{\mathbf{x}} = \left[\mathbf{I} - \begin{bmatrix} \mathbf{D}^{-1}\mathbf{E} & \mathbf{R} \end{bmatrix} \begin{bmatrix} \mathbf{E}^T(\mathbf{D}^{-1})^T\mathbf{P}_x\mathbf{D}^{-1}\mathbf{E} & \mathbf{E}^T(\mathbf{D}^{-1})^T\mathbf{P}_x\mathbf{R} \\ \mathbf{R}^T\mathbf{P}_x\mathbf{D}^{-1}\mathbf{E} & \mathbf{R}^T\mathbf{P}_x\mathbf{R} \end{bmatrix}^{-1} \begin{bmatrix} \mathbf{E}^T(\mathbf{D}^{-1})^T\mathbf{P}_x \\ \mathbf{R}^T\mathbf{P}_x \end{bmatrix} \right] \mathbf{x} = \mathbf{J}_{ex}\mathbf{x} \tag{5}$$

The cofactor matrix for the solution $\mathbf{x}$ is $\mathbf{Q}$. In accordance with the law of error propagation the cofactor matrix $\bar{\mathbf{Q}}$ of the transformed solution $\bar{\mathbf{x}}$ is

Surface Deformation Along the Carmel-Gilboa Fault System by Means of Extended Free Network Adjustment Constraints (9976)
Gilad Even-Tzur (Israel)

FIG Working Week 2019
Geospatial information for a smarter life and environmental resilience
Hanoi, Vietnam, April 22–26, 2019

$$\bar{\mathbf{Q}} = \mathbf{J}_{ex} \mathbf{Q} \mathbf{J}_{ex}^{\mathrm{T}}. \tag{6}$$

6. EXTENDED FREE NETWORK ADJUSTMENT AND GPS NETWORKS

Let us implement the proposed method of extended free network adjustment constraints and extended S-transformation on GPS network and discover how we can define matrixes **D**, **F** and **E**.

GPS vectors define the coordinate differences of the ends of the baseline. GPS vectors are used to determine the relative positions of the network points. They also determine the network datum parameters of orientation and scale. Transformation of a single point from measured GPS coordinates $(x \quad y \quad z)_i$, which contain the datum parameter (denoted by the index w), to coordinates which are stripped from their datum content (denoted by x) is done by three rotations $(r_x \quad r_y \quad r_z)$ and a scale factor (s) as follows:

$$\begin{pmatrix} x_w \\ y_w \\ z_w \end{pmatrix}_i = \begin{pmatrix} s & r_z & -r_y \\ -r_z & s & r_x \\ r_y & -r_x & s \end{pmatrix} \begin{pmatrix} x_x \\ y_x \\ z_x \end{pmatrix}_i = \mathbf{D} \begin{pmatrix} x_x \\ y_x \\ z_x \end{pmatrix}_i \tag{7}$$

The above transformation can also be presented in the following form, which simplifies receiving the **F** matrix:

$$\begin{pmatrix} x_w \\ y_w \\ z_w \end{pmatrix}_i = \begin{pmatrix} 0 & -z_x & y_x & x_x \\ z_x & 0 & -x_x & y_x \\ -y_x & x_x & 0 & z_x \end{pmatrix}_i \begin{pmatrix} r_x \\ r_y \\ r_z \\ s \end{pmatrix} = \mathbf{F}_i \mathbf{y} . \tag{8}$$

As can be seen, vector **y** contains four parameters ($f = 4$). To have $(x_w \quad y_w \quad z_w)^{\mathrm{T}} = (x_x \quad y_x \quad z_x)^{\mathrm{T}}$ the values of the transformation parameters have to be set as, $\mathbf{y}^{\mathrm{T}} = (r_x \quad r_y \quad r_z \quad s) = (0 \quad 0 \quad 0 \quad 1)$, therefore $\mathbf{D} = \mathbf{I}$. Let us assume a network with k points. Then **D** is a $3k \times 3k$ identity matrix and **F** is a $3k \times 4$ matrix as well as **R**. In the case of a GPS network the size of the datum defect is 3 ($d = 3$) and therefore **E** is a $3k \times 3$ matrix with 3 columns for the origin of the network.

7. RESULTS AND CONCLUSIONS

Surface Deformation Along the Carmel-Gilboa Fault System by Means of Extended Free Network Adjustment Constraints (9976)
Gilad Even-Tzur (Israel)

FIG Working Week 2019
Geospatial information for a smarter life and environmental resilience
Hanoi, Vietnam, April 22–26, 2019

The paper focus on extracting the velocity field from monitoring geodetic networks, which were measured by means of GPS. The creation of an accurate and reliable velocity field is based on eight monitoring campaigns that were measured between 1999 and 2016, eight-hour measurement sessions, measuring each network point at least twice in each campaign and using sophisticated mathematical tools. The regional site velocities were estimated with respect to a local datum that was defined by a stable cluster of sites on one side of the fault by means of extended free net adjustment constraints and extended similarity transformation.

The estimation of velocity field was carried out by using the Two-Steps method with an adequate estimation of the variance factor (Even-Tzur, 2004). The first step is accomplished using the Bernese GPS software. The outcome of the software is a minimal constrained solution of the network points and their variance-covariance matrix for each monitoring campaign, referring to a conventional terrestrial coordinate system. By using the extended S-transformation (5) we can strip the datum content of scale and orientations from the measured coordinates. Actually, it can be made directly on the velocities and not on the measured coordinates from each monitoring epoch. Without los of generality, let us consider two measurements epoch, t_1 and t_2. The vector of points positioning in time t_1 is x_1 and in time t_2 is x_2. Therefore, the vector of velocities $\dot{x}$ is

$$\dot{x} = (x_2 - x_1) / (t_2 - t_1) = (x_2 - x_1) / \Delta t . \tag{9}$$

Applying the extended S-transformation and we can get according to eq (5) that $\overline{x}_1 = J_{ex} x_1$ and $\overline{x}_2 = J_{ex} x_2$, then

$$\dot{\overline{x}} = (\overline{x}_2 - \overline{x}_1) / \Delta t = (J_{ex} x_1 - J_{ex} x_2) / \Delta t = J_{ex} (x_1 - x_2) / \Delta t = J_{ex} \dot{x} . \tag{10}$$

The velocity field was calculated related to the Galilee datum. Five points (KABR, GLON, CR02, KBIA and ZPRI) in the north part of the network, which are located mainly in the Lower Galilee region, were selected to define the datum (see Fig. 2). Those points are located far from the DST, where the contribution of the ground displacement due to slip along the DST is expected to be very small. With a 5% level of significance, the five points define a stable datum, which means that there is no significant movement between the datum points. Figure 3 depicts the velocity vectors and their 95% confidence ellipses across the CGFS when compared with

Surface Deformation Along the Carmel-Gilboa Fault System by Means of Extended Free Network Adjustment Constraints (9976)
Gilad Even-Tzur (Israel)

FIG Working Week 2019
Geospatial information for a smarter life and environmental resilience
Hanoi, Vietnam, April 22–26, 2019

the Galilee datum points. The velocity field clearly shows significant velocities in the region under investigation. The horizontal velocity field shows deformations of about 1 mm/yr sinistral.

Points CR05 and CR07 which are ostensibly located on the north-east side of CGFS, show movement similar in direction to points on the south-west side of the faults. The velocity of point CR05 is anomalous with respect to other sites. An examination of the time series of CR05 location does not raise a suspicion of a gross error in one of the monitoring campaigns. However, the unusual velocity of CR05 can be caused additionally by local site effects.

Points which are close to CF, including points CR12 and KRML, show stability relative to the datum points. Points on the west side of the network (KRMV, CR09, ATLT and CR14) show significant movement to the south, indicating a left-lateral sense of slip along the CF of about 1 mm/yr. Those points are not at the same distance from the fault and they are located on the western slopes of Mount Carmel except ATLT, which is located at the sea sandstone (Kurkar) ridge by the beach.

The point MRKA and the nearby point CR13 show no significant velocities and neither does KRTV, although located close to them on the other side of the fault, relative to the datum sites, but their insignificant velocities point to the same direction. Points CR07 and CR16, which are located at the edge of the Yizre'el Valley on both sides, express the same velocity in the same direction. The velocity of GILB, which is expected to be affected the most by ground displacement due to slip along the DST, shows velocity that is appropriate to a sinistral movement along the GF.

The insignificant velocities of MRKA and KRTV relative to the Galilee datum and the significant velocities of CR16 and CR07 may indicate that the southern segment of CF is not active. One can suggest that the velocities in the Yizre'el Valley region are due to activities along the GF or similar trending faults, which are halted by the Tivon Hills.
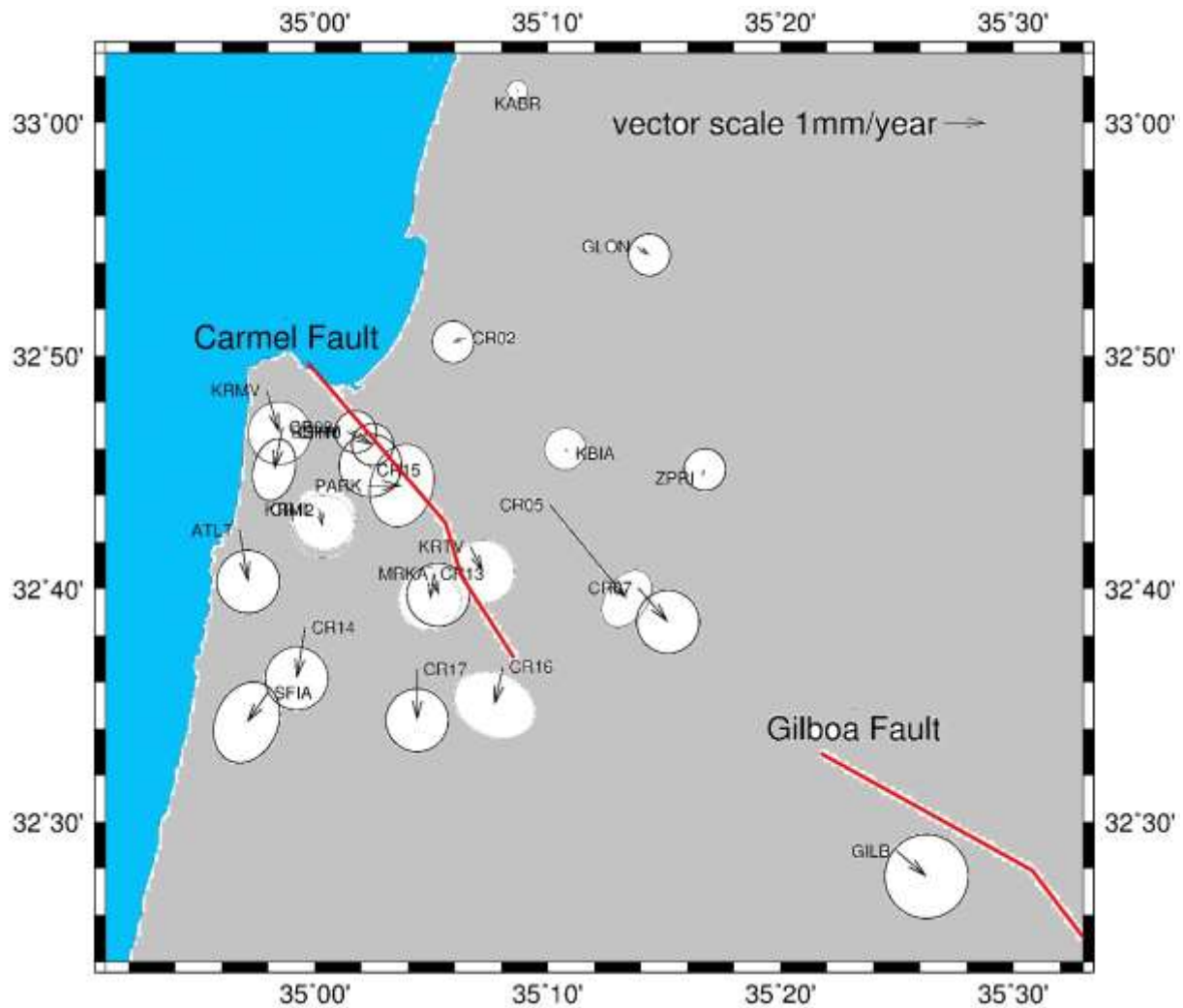
Surface Deformation Along the Carmel-Gilboa Fault System by Means of Extended Free Network Adjustment Constraints (9976)
Gilad Even-Tzur (Israel)

FIG Working Week 2019
Geospatial information for a smarter life and environmental resilience
Hanoi, Vietnam, April 22–26, 2019

Figure 3. The velocity vectors and their 95% confidence ellipses across the Carmel-Gilboa Fault System (CGFS) relative to the Galilee datum defined by points KABR, GLON, CR02, KBIA and ZPRI Analysis is based on eight measuring campaigns carried out between 1999 and 2016. Red lines denote the geological fault traces.

REFERENCES

Baarda, W., 1973. S-Transformation and criterion Matrices. Netherlands Geodetic Commission, Publication on Geodesy, New Series, Vol. 5, No. 1.

Dach, R., Lutz, S., Walser, P., Fridez, P., 2007. Bernese GNSS Software Version 5.2. Astronomical Institute, University Bern, http://www.bernese.unibe.ch/docs/DOCU52.pdf.

Even-Tzur, G., 2004. Variance Factor Estimation for Two-Step Analysis of Deformation Networks. Journal of surveying engineering. Journal of Surveying Engineering, 130(3):113-118.

Surface Deformation Along the Carmel-Gilboa Fault System by Means of Extended Free Network Adjustment Constraints (9976)
Gilad Even-Tzur (Israel)

FIG Working Week 2019
Geospatial information for a smarter life and environmental resilience
Hanoi, Vietnam, April 22–26, 2019

Even-Tzur, G., 2011. Deformation Analysis by Means of Extended Free Network Adjustment Constraints, Journal of Surveying Engineering 137, 47–52.

Even-Tzur, G., 2012. Extended S-Transformation as a Tool for Deformation Analysis, Survey review 44, 315–318.

Even-Tzur, G. and Reinking, J., 2013. Velocity field across the Carmel fault calculated by extended free network adjustment constraints. Journal of Applied Geodesy, 7(2), pp.75-82.

Fleischer, L. and Gafsou, R., 2005. Structural map on top Judea Group. In: Hall, J.K., Krasheninnikov, V.A., Hirsch, F., Benjamini, Ch., Flexer, A. (eds.), Geological Framework of the Levant, Plates (Plate V). Historical Productions-Hall, Jerusalem.

Hofstetter, A., van Eck, T., Shapira, A., 1996. Seismic activity along the fault branches of the Dead Sea –Jordan transform: the Carmel–Tirtza fault system. Tectonophysics, 267, 317–330.

Papo, H., 1985. Extended free net adjustment constraints. Bull. Géodésique, 59(4), 378–390.

Papo, H., 1986. Extended free net adjustment constraints. NOAA Technical Report NOS 119 NGS 37, 16.

Rotstein, Y., Shaliv, G., Rybakov, M., 2004. Active tectonics of the Yizre'el valley, Israel, using high-resolution seismic reflection data. Tectonophysics 382, 31–50.

Segev, A., Lyakhovsky, V. and Weinberger, R., 2014. Continental transform–rift interaction adjacent to a continental margin: The Levant case study. Earth-Science Reviews, 139, pp.83-103.

Segev, A. and Rybakov, M., 2011. History of faulting and magmatism in the Galilee (Israel) and across the Levant continental margin inferred from potential field data. Journal of Geodynamics, 51(4), pp.264-284.

Segev, A., Rybakov, M., Lyakhovsky, V., Hofstetter, A., Tibor, G., Goldshmidt, V., Ben-Avraham, Z., 2006. The structure, isostasy and gravity field of the Levant continental margin and the southeast Mediterranean area. Tectonophysics 425, 137–157.

Wolf, H., 1977. Eindeutige und mehrdeutige Geodätische Netze. Adh. Braunschw. Wiss. Ges., Band 28.

CONTACTS

Gilad EVEN-TZUR
Mapping and Geo-Information Engineering,
Faculty of Civil and Environmental Engineering
Technion - Israel Institute of Technology
Technion City, Haifa 32000
ISRAEL
Email: eventzur@technion.ac.il

Surface Deformation Along the Carmel-Gilboa Fault System by Means of Extended Free Network Adjustment Constraints (9976)
Gilad Even-Tzur (Israel)

FIG Working Week 2019
Geospatial information for a smarter life and environmental resilience
Hanoi, Vietnam, April 22–26, 2019